



Hassouna, S., Ur Rehman Kazim, J., Rains, J., Jamshed, M. A., Ur Rehman, M., Imran, M. A. and Abbasi, Q. H. (2023) Indoor Field Trials for RIS-aided Wireless Communications. In: 2023 IEEE International Symposium on Antennas and Propagation and USNC-URSI Radio Science Meeting, Portland, Oregon, USA, 23–28 July 2023, pp. 75-76. ISBN 9781665442282.

There may be differences between this version and the published version. You are advised to consult the publisher's version if you wish to cite from it.

<https://eprints.gla.ac.uk/294749/>

Deposited on: 21 March 2023

Enlighten – Research publications by members of the University of Glasgow  
<https://eprints.gla.ac.uk>

# Indoor Field Trials for RIS-aided Wireless Communications

Saber Hassouna, Jalil ur Rehman Kazim, James Rains, Muhammad Ali Jamshed, Masood Ur Rehman, Muhammad Ali Imran, and Qammer H. Abbasi

James Watt School of Engineering, University of Glasgow, Glasgow, U.K

Email: s.hassouna.1@research.gla.ac.uk

**Abstract**—Recently, both academics and industry have paid close attention to the potential of adopting the prototyping of a Reconfigurable Intelligent Surface (RIS)-aided wireless communication. In this paper, we present a novel RIS prototype operating in the 3.75 GHz range with 4096 configurable elements. We propose a realistic receiver-RIS Wi-Fi feedback link and an effective method for configuring the RIS over the air by taking advantage of the geometrical array features. Our 1-bit RIS prototype offers an 18 dB power gain over the case when it is replaced with a metal plate. The indoor measurements have been carried out where the transmitter and receiver are separated by a concrete wall.

## I. INTRODUCTION

Recent years have been a rapid expansion of research into wireless communications employing reconfigurable intelligent surfaces (RISs). New wireless transceiver architectures have been realized using RISs, which may result in a paradigm change in transceiver design and lower the hardware cost of next wireless communication systems. In addition, RISs can modify the environment for electromagnetic wave propagation [1]. Consequently, it is worth mentioning that RIS might be deployed much more widely across the wireless network, due to its inexpensive price, to effectively modify signal propagation. There has been a significant amount of research on the theoretical modelling of the RIS, however there are currently relatively few test-bed systems that have been developed to assess the RIS's functionality in a real-world setting [2]. The main contributions of our research are as follows:

- We have developed and tested a unique feedback-based adaptive reflection coefficient optimization algorithm that enables smart reflection without changing the current communication standards.
- We have performed indoor non-line-of-sight (NLoS) trials and demonstrated an 18 dB channel gain improvement compared to a metal plate reference case.

The RIS implementation, beamforming and simulation results are presented under RIS-assisted wireless communication systems in section II.

## II. RIS-ASSISTED WIRELESS COMMUNICATION SYSTEMS

This section describes the prototype of the RIS-aided wireless communication system seen in Fig. 1, which is made up of Personal Computers (PCs), Universal Software Radio Peripherals (USRPs), a RIS, and the real-time RIS-UE feedback module. The key parts of the transmitter are the host computer,

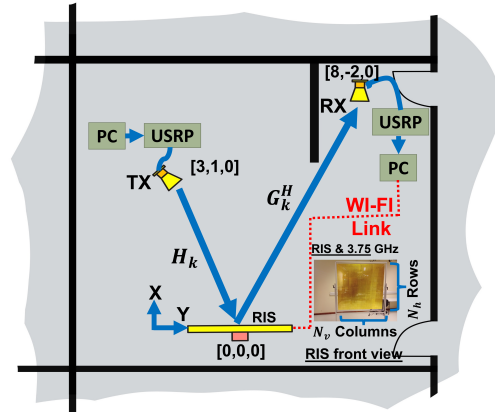


Fig. 1. Indoor Measurement Setup at MAST Lab

a USRP, and an antenna. The receiver has the same essential parts. These transceivers represent a user equipment (UE) and an access point (AP) or base station (BS), respectively. The locations of the Transmitter, Receiver and RIS are measured in metres. A single passive antenna on the transmitter is used to transmit 64-subcarriers OFDM signal. The USRP is used to transport the data. The receiver decodes the data stream, and the host computer recover the transmitted OFDM signal.

### A. Implementation

The fabricated RIS has a 64x64 elements grid with a square size of 192 cm x 192 cm. The front view of the RIS board is shown in Fig. 1. We have created a 1-bit prototype with a phase difference between the two states of about 180 degrees. A continuous OFDM Transmission is tested with Two Ettus Research Universal Software Radio Peripheral (USRP) X300 at the transmitter and receiver connected with standard horn antenna for each of them. Fig. 2 shows the RIS response of the entire band around the centre frequency. The gap of the response between the switched-off state and the achieved gain is large and this reveals the remarkable gain improvement that can be obtained by the RIS technology.

### B. RIS-aided Beamforming

The RIS will either scatter or reflect the incident wave depending on its configurations. The Signal-to-Noise Ratio (SNR) measures the communication performance where both transmitter and receiver are equipped with a horn single-antenna as per Fig. 1. Consequently, the RIS can help the

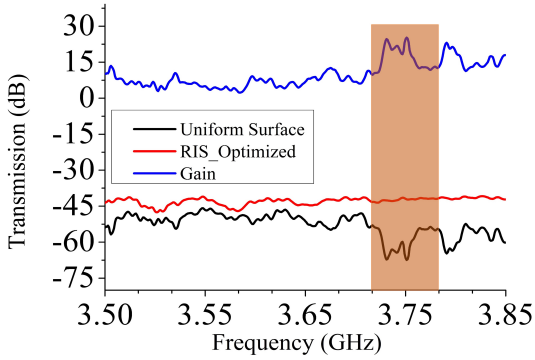


Fig. 2. Measured Transmission Response when RIS is unconfigured, Optimized state and achieved gain

communication system by maximizing the power of the received signal by optimizing its reflection coefficients. The 2D-DFT codebook is still consistent with the structure of the optimal RIS phase shifts for a given incident angle and a specified reflecting angle [3]. The received signal  $y_k \in \mathbb{C}$  can be represented as follows:

$$y_k = \left( (G_k \odot H_k)^T w_\theta + h_d \right) x_k + n_k \quad (1)$$

where  $x_k \in \mathbb{C}$  is the transmitted signal,  $\odot$  denotes the Hadamard product and  $n_k \sim \mathcal{CN}(0, \sigma_n^2)$  is the white Gaussian noise with variance  $\sigma_n^2$ . The vector  $w_\theta \in \mathbb{C}^N$  contains the actual reflection coefficients of the RIS that determine the amplitude losses and phase shifts. The end-to-end power gain without the direct path can be presented as:

$$\left| (G_k \odot H_k)^T w_\theta \right|^2 = \beta_a \beta_b \left| a(\varphi_{\beta_a}, \theta_{\beta_a}) \odot a(\varphi_{\beta_b}, \theta_{\beta_b}) w_\theta \right|^2 \quad (2)$$

where  $\beta_a \geq 0$  and  $\beta_b \geq 0$  are the pathlosses from the AP to the RIS and from the RIS to the user respectively.  $a(\varphi, \theta)$  is the steering vector while  $\varphi$  and  $\theta$  are the azimuth and elevation angles respectively. The best approach chooses phase-shifts such that all RIS elements' reflected signals arrive in phase to the receiver. The optimal phase vector  $w_{\theta_c} = \underset{|w_\theta|_i=1}{\operatorname{argmax}} \left| (G_k \odot H_k)^T w_\theta \right|^2$  can be approximated by the columns of the DFT matrix when the RIS surface is large. Consequently, each column of the codebook beamform  $W_{\theta_N} = F(N_v) \otimes F(N_h) \in \mathbb{C}^{N \times N}$  can be a possible reflection configuration for an incident signal in a certain beam direction. Let  $\otimes$  denotes the Kronecker product. We searched in the codebook for the best configuration that maximize the received signal power in (1).

### C. Simulation Results

Fig. 3 shows the measurements of the received signal power against different configurations at 3.75 GHz. It is compared with the received power when the RIS surface is unconfigured. Algorithm 1, using the feedback iterations, searches in the codebook  $\{W_{\theta_N}\}$  for the configuration that increases the received signal power. It is noticed that there are some

### Algorithm 1 DFT Codebook Algorithm

- 1: Initialize the configuration vector  $w_{\theta_0} \in \mathbb{C}^{N \times 1}$  from the codebook  $\{W_{\theta_N} \in \mathbb{C}^{N \times N}\}$
- 2: Receive initial feedback of the RX signal power  $y_0$ .
- 3: Search in the codebook  $W_{\theta_N}$
- 4: **for**  $w_{\theta_n}$ ,  $n \in [1, N]$  **do**
- 5:  $w_{\theta_N} \leftarrow [w_{\theta_1}, w_{\theta_2}, \dots, w_{\theta_N}]$  where  $w_{\theta_n}$  is the  $n$ -th column of the codebook matrix  $W_{\theta_N}$ .
- 6: Receive the signal power  $y_n$  using configuration  $w_{\theta_n}$
- 7: **if**  $y_{n-1} \geq y_n$  **then**
- 8:  $w_{\theta_n} \leftarrow w_{\theta_{n-1}}$
- 9: **end if**
- 10: **end for**
- 11: Evaluate the received signal power with the new configuration.

configurations in the codebook that gives the same power gain and this explains the flat response in Fig. 3 at certain configurations. A power enhancement of 18 dB is obtained and this reveals the benefits of RIS technology in wireless communications.

### D. CONCLUSION

RIS is a promising technology and efforts are recommended towards test-bed implementations in order to demonstrate real and actual communication models.

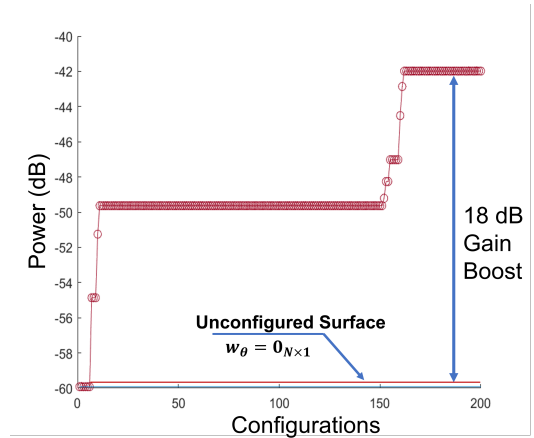


Fig. 3. Signal Power Measurements at 3.75 GHz.

### REFERENCES

- [1] W. Tang, M. Z. Chen, X. Chen, J. Y. Dai, Y. Han, M. Di Renzo, Y. Zeng, S. Jin, Q. Cheng, and T. J. Cui, "Wireless communications with reconfigurable intelligent surface: Path loss modeling and experimental measurement," *IEEE Transactions on Wireless Communications*, vol. 20, no. 1, pp. 421–439, 2020.
- [2] J. Rains, A. Tukmanov, T. J. Cui, L. Zhang, Q. H. Abbasi, M. A. Imran *et al.*, "High-resolution programmable scattering for wireless coverage enhancement: an indoor field trial campaign," *IEEE Transactions on Antennas and Propagation*, 2022.
- [3] X. Pei, H. Yin, L. Tan, L. Cao, Z. Li, K. Wang, K. Zhang, and E. Björnson, "Ris-aided wireless communications: Prototyping, adaptive beamforming, and indoor/outdoor field trials," *IEEE Transactions on Communications*, vol. 69, no. 12, pp. 8627–8640, 2021.